Optimizing Baffle Length for Mixed Convective Flow Within a Ventilated Square Cavity with Discrete Heat Sources Mounted at Side Walls

Saad Been Mosharof [a), b)], HM Toufik Ahmed Zisan [a), b)] *, Tahmidul Haque Ruvo [a), b)], and Md. Mahmud-Or-Rashid [a), b)]

a) Department of Mechanical Engineering, Shahjalal University of Science and Technology, Sylhet 3114, Bangladesh.

b) Department of Mechanical Engineering, Bangladesh University of Engineering and Technology, Dhaka 1000, Bangladesh.

Abstract

Mixed convection within a ventilated square cavity having baffle at the bottom wall and heating elements at the side walls has been analyzed. The inlet opening has been set at the bottom of the left wall while the exit opening is put at the bottom of the right wall. Considering air (Pr = 0.71), dimensionless and steady form of mass, momentum and energy equations are solved by implementing proper boundary condition with the help of Galerkin method based finite element scheme. Maintaining pure mixed convection (Ri = 1), baffle length is changed from 0 to 0.95L and heaters location is varied from 0.1L to 0.7L across Re = 10 to 1000. Qualitative changes of the domain are observed with the help of streamline and isothermal plots. For quantitative comparison, average temperature, Nusselt number, pressure drop and performance index has been considered. Counteracting effects of the increase in Nusselt number and pressure drop are accounted together with the help of performance index which yielded the most economic and optimum baffle height and heaters location. Final evaluation shows that the optimum length of the baffle and the position of the heaters can perform most effectively in the range of Re = 20 – 400.

Keywords: Mixed Convection; Baffle; Vented Cavity; Discrete Heating Element; Performance Index.

1. Introduction

Over the years various technologies have developed which produce a significant amount of heat during their operations. This heat is to be removed from the equipment in an efficient manner so that the equipment can run in its desired range. Heat transfer by the help of convection is a long-

used heat removal procedure in various engineering applications e.g., solar energy collectors, heat exchangers, nuclear reactor cooling, electronic package cooling etc. Special attention is being provided to the cooling of electric circuits and chips. With the diminishing size of electronic equipment and chips, much heat per area is being generated. To efficiently remove this heat, many techniques are being devised through research works. In the convection process heat is taken away from the material with the help of bulk fluid advection and molecular diffusion process. In case of natural convection, flow is governed by buoyancy force which is created due to change in density of the material due to heating. For forced convection, flow is predominantly governed by the flow inertia. Fluid gets powered by external fan or blower etc. [1]. For mixed convection, flow is a compromise between buoyancy force and flow inertia. Both of these forces equally dominate the convection process.

Natural convection in rectangular, triangular and trapezoidal cavities has long been studied [2–10] to improvise the heat transfer by this low-cost process. However, this process is of no avail when a significant amount of heat transfer is required. In such cases use of mixed or forced convection is a good choice (e.g., cooling of electronic packages, chip cooling, ventilation, reactor vessel cooling, air conditioning etc.). Mixed convection has gained a lot of attention due to its significant improvement over natural convection in terms of heat transfer and comparatively lower cost in comparison to forced convection.

Raji and Hasnaoui [11] performed numerical investigation to analyze the optimum inlet and exit configuration over a range of Reyleigh number (10^3 to 5×10^6) for rectangular cavity. It was opined that the bottom inlet and top exit configuration works well whenever the heater wall is side mounted. In case of cavity with vertical entry (at top or bottom), vertical exit (at bottom or top) and a side mounted isothermal heater, heat transfer was found to be increasing in case of aiding flow while a decrease is found in case of opposing flow [12]. In a combined experimental and numerical study for arc shaped cavity with top lid moving in horizontal direction, Chen and Cheng [13] found that, local Nusselt number across the lid increases with the increase value of Grashof number. For $Gr \geq 10^6$, local Nusselt number is significantly improved due to the buoyancy effect. However, at the transition regime between laminar and turbulent flow, the setup faces a severe reduction in heat transfer accompanied by a steep change in flow pattern. Saha et al. [14] numerically found the optimum inlet and exit configuration for a rectangular enclosure with side mounted isoflux wall at $Re = 100$ and across the range $Ra = 0$ to 10. Heat transfer through air in vented cavity was found to

be affected by the aspect ratio of the cavity and placement of heater [15]. Rahman et al. [16] analyzed mixed convection in an open channel along with the application of magnetic field (Hartmann number 0 to 20). Increased effect of magnetic field reduced the size of vortex generated due to buoyancy effect and it also affected thermal boundary layer development. It also reduced the average value of Nusselt number. Through experimental study on a multi-vented enclosure having three flush mounted heater at the bottom, Ajmera and Mathur [17] concluded that element with highest heat flux should be placed near the entry of the cavity in cases of high Reynolds number operation at all Grashof numbers. For a simulation of nanofluid undergoing mixed convection in a square cavity, Garoosi et al. [18] obtained that at low Rayleigh number and higher values of Richardson numbers single phase models can be implemented to study such heat transfer behavior. Through a rigorous numerical analysis for mixed convection by the Lattice Boltzmann method, Burgos et al. [19] found that at $Ri = 1$ and at higher values of Reynolds number (> 200), flow was stratified within an open top cavity. With the increase in the Richardson number, flow became unsteady and unstable. Mehryan et al. [20] numerically demonstrated that, for mixed convection within a square cavity having a heated oscillating cylinder, heat transfer rate increased with increased frequency (1 – 48 Hz). However, increase in amplitude does not always guarantee an increase in heat transfer. For mixed convection within a lid driven square cavity with a porous heat source [21], an increase in heat transfer was observed in the range of Ri = 0.1 to 1 since the flow regime near the source was greatly affected by the buoyancy force. However, a decrease in Nusselt number was observed for Ri = 1 to 10. Ruvo et al. [22] investigated the effect of inflow conditions for pure mixed convection (Ri = 1) in an open T-shaped cavity and found that uniform inflow condition provided better heat transfer performance over the Poiseuille and Couette inflow conditions.

Placement of baffle inside mixed convection flows is an interesting concept for enhancing heat transfer. Baffles usually hinders the flow within the cavity or channel, causes recirculation of fluid and in the process it can also direct fluid to any specific direction for enhancing the removal of heat from any heated source. Kotcioglu et al. [23] experimentally analyzed the effect of wing type vortex generator in a rectangular channel across Re = 3000 to 30,000. Winglets were inclined at different angles ranging from 7° to 20°. These angles seemed to affect the rate of heat transfer. Use of porous baffles in rectangular channels provided a 300% increase in heat transfer but also caused an increase in pressure drop. Numerical explorations were done by Valencia and Sen [24]

to find best periodic vortex generator in a parallel channel. Placement of two square bars within the flow domain provided best possible heat transfer at Re = 800. In an experimental investigation, Karwa et al. [25] found out that porous baffles perform better in comparison to solid baffles with respect to friction factor and heat removal. Porous baffles showed an increase in heat transfer performance ranging from 45 to 60.6% and an increase in friction factor by 2.3 to 3.0 times in comparison to the smooth duct without any baffles. For solid baffles, despite an increase in heat transfer performance by 73.7 to 82.7%, the friction factor increased significantly to up to 9.6 to 11.1 times. For a vertical mixed convective channel having a heat generating element in the center, Radhakrishnan et al. [26] showed that the placement of baffle at the midpoint of the bottom wall could give a maximum amount of heat transfer. This result was also recreated in an experiment to validate the simulation. Belmiloud and Chemloul [27] demonstrated that even number of baffles provided good heat transfer opportunities whenever flow occurred through a rectangular channel having an isoflux bottom wall with a bottom entry and top exit configuration. On the other hand, in case of bottom entry and bottom exit configuration, odd number of baffles performed better in the range of $2 \leq Ri \leq 7$. Through a numerical analysis by Sharma et al. [28] opined that, the placement of a baffle within the flow path of a grooved rectangular channel improved heat exchange in case of both assisting and aiding flow. At Re = 200 and $Ri \leq 1$, the presence of baffles caused 25–175% increase in heat transfer. Sahel et al. [29] showed low heat transfer zones can be avoided or removed to aid in increased heat transfer with the optimal use of perforated baffles in a rectangular channel. Belmiloud et al. [30] numerically analyzed the effect of baffle length in a vertical rectangular channel. An increase in Nusselt number was observed with the increase in baffle length varying from 0.3 to 0.7 for a fixed Grashof number of 10^4 and a range of Reynolds number from 50 to 500. A thorough numerical analysis of a rectangular air filled (Pr = 0.71) cavity having a centrally located baffle at different arrangements, performed by Gokulavani et al. [31] disclosed that the vertical orientation of the baffle yielded a high value of heat transfer. In this experiment across Rayleigh numbers 10^3–10^6 and Reynolds numbers 10, 100 and 500, it was also observed that, bottom entry and bottom exit within the cavity provided maximum heat transfer within the open cavity for any orientation of baffle. Alhussain [32] numerically studied the mixed convection in a multi-pored square cavity for varying baffle positions with discrete heating elements in the top and bottom walls. He observed that the heat transfer performance enhanced when the baffle was placed closer to the outlet pores for Ra varying in the range of 10^5 to 10^6. Similarly, Rehman et al. [33]

discussed the effect of different inner obstacle shapes on the mixed convection inside a square-vented enclosure and showed that triangular obstacles performed better over circular and rectangular ones. On the other hand, fluid-structure interaction in a lid-driven square cavity was explored numerically by Mahmood et al. [34]. Their exploration revealed that the placement of elastic adiabatic fin inside the cavity helped in the formation of complete vortices in the flow domain, and along with this benefit, 73.8% enhanced heat transfer could be achieved for Re = 300 compared to Re = 100.

Aforementioned literature review suggests that a considerable effort has already been put forward by researchers for increasing heat transfer in mixed convection. However, none of the studies considered the combined effect of variable position and height of the baffle in the mixed convective heat transfer. Though many individuals separately analyzed the effect of the size and orientation of the baffle, no one included the economic consideration in their study. Thus, current study tries to excel the research in a different aspect. This numerical analysis will be conducted keeping in mind the factors of thermal performance and pressure drop within the flow domain. A novel approach of combining these two factors in a mathematical term called 'performance index' is implemented in the current geometry to find the most economic and most optimum baffle height and heater location for different operating range of the governing parameters.

2. Physical Modelling

Two-dimensional ventilated square cavity considered for the current analysis is shown in Fig. 1. Sides of the cavity are considered of length, L. Two isothermal heaters of length 0.2L are placed symmetrically at two side walls. Cold fluid (air, Pr = 0.71) enters through the inlet situated at the bottom of left wall and after removing heat from the heaters exits through the bottom of right wall. Both inlet and exit have equal height of 0.2L. Remaining portion of the walls of enclosure are considered adiabatic. An adiabatic baffle (of height, H and width, 0.1L) is placed at the center point of bottom wall in order to obstruct the flow of fluid and move it across the heaters.

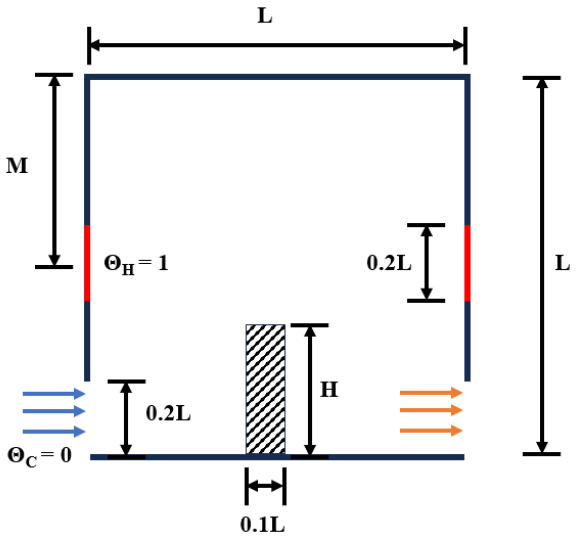

Fig. 1: Geometry of the current study (color online).

3. Mathematical Modelling

Mathematical formulation for the current problem assumes a steady, laminar and incompressible flow. To account for the density variation, Boussinesq approximation is considered throughout the problem. Non-dimensional form of the mass transfer, momentum transfer and energy flow equations are listed below:

$$\frac{\partial U}{\partial X}+\frac{\partial V}{\partial Y}=0, \tag{1}$$

$$U\frac{\partial U}{\partial X}+V\frac{\partial U}{\partial Y}=-\frac{\partial P}{\partial X}+\frac{1}{Re}\left(\frac{\partial^2 U}{\partial X^2}+\frac{\partial^2 U}{\partial Y^2}\right), \tag{2}$$

$$U\frac{\partial V}{\partial X}+V\frac{\partial V}{\partial Y}=-\frac{\partial P}{\partial Y}+\frac{1}{Re}\left(\frac{\partial^2 V}{\partial X^2}+\frac{\partial^2 V}{\partial Y^2}\right)+Ri\Theta, \tag{3}$$

$$U\frac{\partial \Theta}{\partial X}+V\frac{\partial \Theta}{\partial Y}=\frac{1}{RePr}\left(\frac{\partial^2 \Theta}{\partial X^2}+\frac{\partial^2 \Theta}{\partial Y^2}\right), \tag{4}$$

where, the mentioned equations use the reference values as follows:

$$P=\frac{p}{\rho u_{in}^{\ 2}},(U,V)=\frac{(u,v)}{u_{in}},\Theta=\frac{T-T_c}{T_h-T_c},. \tag{5}$$

In equation 5, *U*, *V* represents dimensionless velocity along X axis and Y axis respectively. *P* denotes non-dimensional pressure while Θ indicates non-dimensional temperature.

Parameters governing the problem are Richardson number (*Ri*), Reynolds number (*Re*) and Prandtl number (*Pr*) [35]. Their expressions are mentioned below:

$$Ri = \frac{g\beta\Delta TL}{u_{in}^2}, Re = \frac{u_{in}L}{\upsilon}, Pr = \frac{\upsilon}{\alpha} \tag{6}$$

In the above expression, υ represents kinematic viscosity, α denotes thermal diffusivity and β indicates coefficient of volume expansion.

After solving the governing equations (1-4) the results are analyzed qualitatively and quantitatively. For quantitative scrutinization, following performance parameters are considered.

Non-dimensional average temperature is used to visualize the overall temperature rise within the flow domain.

$$\Theta_{avg} = \frac{1}{A}\int_A \Theta dA \tag{7}$$

Heat transfer performance has been evaluated by using total average value of Nusselt number. It is found by summing the average of the Nusselt number across both isothermal heaters.

$$Nu = Nu_{avg,left} + Nu_{avg,right} = \frac{1}{0.2L}\left(\int_{0.4L}^{0.6L}\left.\frac{\partial\Theta}{\partial X}\right|_{left} dY + \int_{0.4L}^{0.6L}\left.\frac{\partial\Theta}{\partial X}\right|_{right} dY\right) \tag{8}$$

Calculation of pressure drop is used to signify the effect of baffle on the power required to continue the motion of fluid through the cavity.

$$\Delta p = p_{in} - p_{out} \tag{9}$$

To simultaneously compare the combined effect of heat transfer enhancement and increase in pressure drop due to the introduction of baffle, performance index [36] is calculated for each case.

$$\eta = \frac{Nu_{\text{with baffle}} \big/ Nu_{\text{without baffle}}}{\Delta p_{\text{with baffle}} \big/ \Delta p_{\text{without baffle}}} \tag{10}$$

Non-dimensional form of the conditions set at boundary for the ongoing study is given in Table 1.

Table 1: Non-dimensional boundary conditions

Boundary Ends	Temperature	Velocity
Isothermal heaters	$\Theta_H = 1$	$U = 0$, $V = 0$

Inlet	$\Theta_C = 0$	$U = 1, V = 0$
Remaining surfaces	$\partial\Theta/\partial N = 0$	$U = 0, V = 0$

4. Numerical Method and Validation

Governing equations stated in the previous section are solved by employing the Galerkin method based finite element scheme. 'COMSOL Multiphysics 6.1' has been used to solve the governing equation. In this procedure, the partial differential form of the governing equations is at first converted into 'weak form' which is an integral form of the previous equations. Then after subdividing the working domain into multiple smaller elements, the weak form of equations is applied on each of these elements with the help of 'basis' functions. Following that system of equations for the entire domain is solved iteratively using the provided boundary conditions. The dependent variables (U, V, P and Θ) are considered to be solved when the relative error maintains a threshold of $\gamma_{i+1} - \gamma_i < 10^{-5}$, where γ indicates individual dependent variables and i denotes number of iterations. Solutions are obtained each nodal points which after being combined gives solution for the entire domain.

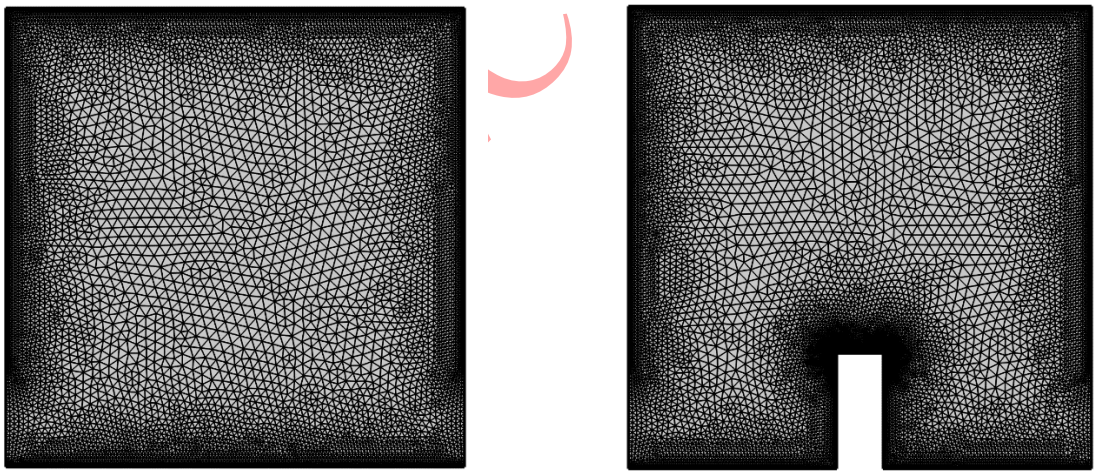

(a) (b)

Fig. 2: Segregation of the computational domain for (a) system with no baffle, (b) system with a baffle of $H = 0.25L$

Fig. 2 shows the mesh systems considered in the current study. Triangular mesh elements are considered within the overall flow domain while quadratic mesh elements are utilized at the boundary regions. Since unstructured triangular mesh causes higher numerical diffusion and the

surface regimes are more anisotropic, quadratic meshing is preferable here. Alongside, element density is significantly increased at the boundary regions in order to improve the accuracy of the result. On the other hand, the extra diffusion of triangular meshing elements is utilized in the bulk flow domain for getting faster convergence. A thorough grid independence test (Fig. 3) has been conducted to find out the most optimum number of elements for conducting the numerical study. The plot shows variation of average value of the temperature of fluid domain for different number of elements. In case of system with no baffle, result becomes almost constant after an element number of 17608 while for the representative case of system with baffles (here $H = 0.25L$) the result stops showing any significant variation after an element number of 21610. Both of these cases utilize finer mesh elements within the main flow domain and extremely fine mesh elements at the boundary regions.

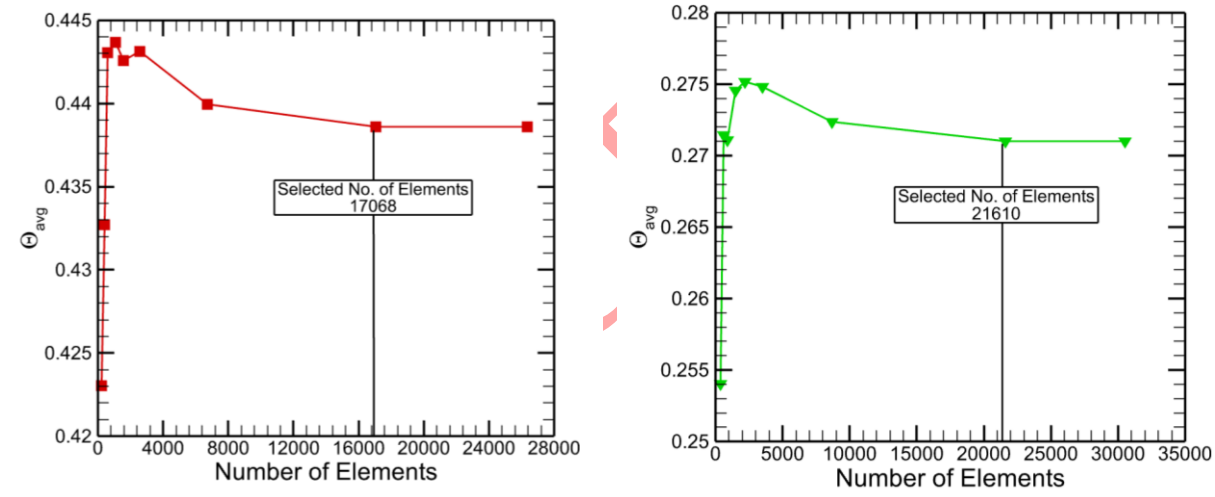

(a) (b)

Fig. 3: Grid independence test for (a) system with no baffle, (b) system with a baffle of $H = 0.25L$ at $Re = 100$ and $Ri = 1$

To find out the validity of the present code, it has been used to recreate the work of Singh and Sharif [9]. In that numerical study convective flow in an open cavity was studied for different inlet and exit configuration. A quantitative plot of average fluid temperature (air) for a range of Richardson number is redrawn. Current code is used to regenerate the work $Re = 100$ and $Re = 300$ in the configuration A (top inlet and top exit). It is seen that the current code can quiet clearly predict the heat transfer behavior for the natural, mixed and forced convection regimes of heat transfer. This similarity indicates the accuracy of the current code.

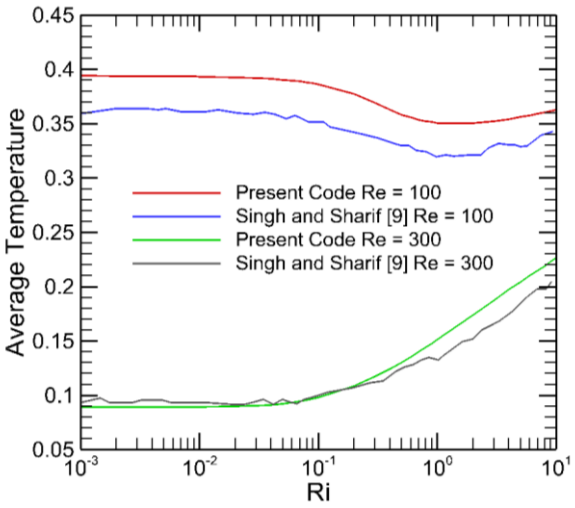

Fig. 4: Quantitative validation of the present code with the study of Singh and Sharif [9] (color online).

5. Results and Discussion

For current study, the effect of baffle height and location of the discrete heaters on the performance of mixed convective heat transfer has been numerically investigated for a wide range *Re* (10 to 1000) and *Gr* (100 to 10^6) while maintaining the *Ri* constant at unity. The analysis is conducted by varying the baffle height from 0 to 0.95*L* and locating the heaters from 0.1*L* to 0.7*L*. For both of the cases, their impact on the thermal and hydraulic performance is observed. First of all, the streamlines and isotherms are plotted to qualitatively visualize the combined effect of the variation of baffle height, heater's location and Reynolds number on the transfer behavior. Later, the combined effect is quantitatively examined using average temperature of the domain, average value of Nusselt number, drop in pressure and performance index. Finally, the optimum baffle height, heater's location and flow condition are determined by interpreting the entire range of data.

5.1 Analysis of The Flow Field

First of all**,** to visualize the flow behavior of the system, streamlines are plotted, as depicted in Fig. 5, for different combinations of *Re* and *H* while keeping *M* = 0.5*L*. It is noted that the increase of baffle height reduces the recirculation of the working fluid but redirects toward a longer path from inlet to exit. The delayed and redirected flow becomes more inclined along the heat generating elements and results in an enhanced heat transfer performance. On the other hand, when

Re increases, both the mass flow rate and vortex formation increase in the flow domain. The prominent effect of increased mass transfer greatly enhances the heat transfer performance. Also, it can be noted that the streamlines get more inclined with the right wall as the *Re* increases. This phenomenon excels the heat removal rate from the heating element placed at the right wall. In particular, for low Reynolds number (Re = 50) and no baffle (H = 0) condition, vortices are formed close to the heating elements and the flow gets separated into two parts, one taking away some heat in the exit and the other one getting recirculated. This behavior of the flow reduces the overall heat transfer performance along with the reduction in pressure drops for not using any baffle. To analyze the other side of the fence, another case can be considered with maximum baffle height (H = 0.95L) and highest Reynolds number (Re = 1000). The increased mass transfer rate due to high *Re* amplifies the heat transfer rate. Besides, the amplification is greater for right-walled element since the flow is more inclined with the right wall and slightly separated along the left wall. However, the overall economy of the heat transfer may be reduced due the pronounced pressure drops caused by the flow obstruction of the baffle.

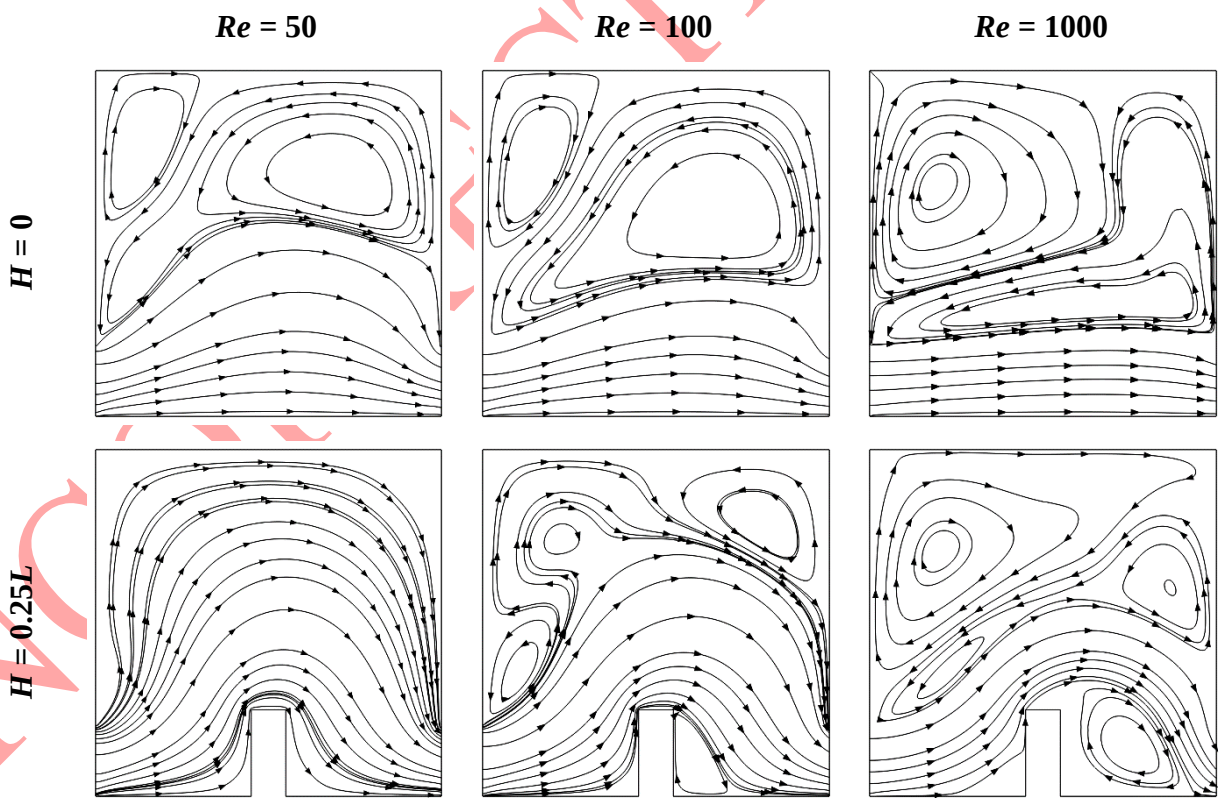

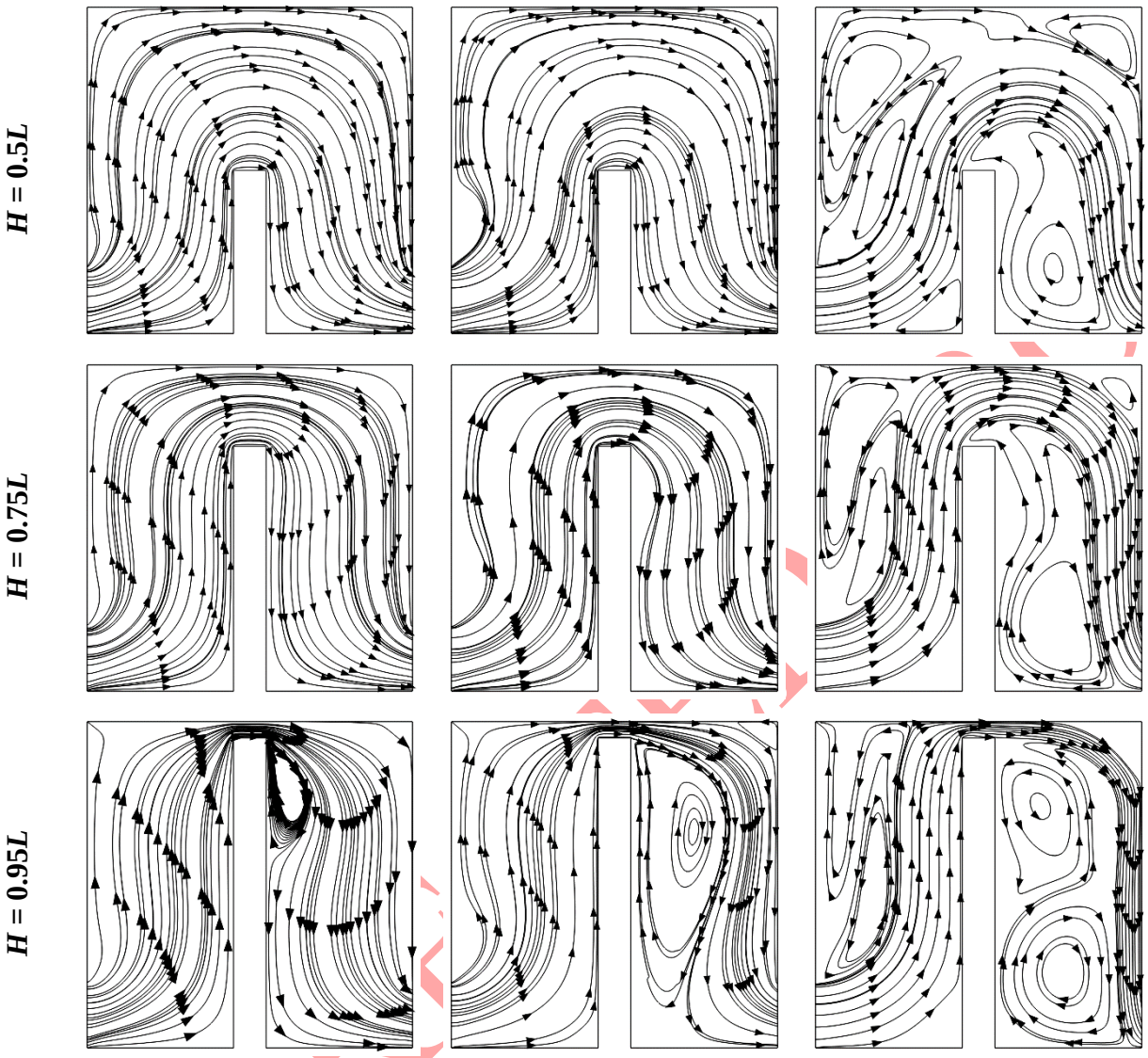

Fig. 5: Illustration of flow field for several combinations of Reynolds number and baffle height (color online).

Similarly, the effect of heaters location at a fixed baffle height (H = 0.55L) on the streamlines are shown in Fig. 6. A close speculation confirms that a slight variation in the streamlines pattern occurs with the change of heaters location. When heaters are placed at the closest vicinity of the inlet, bulk fluid takes the heat earlier, and the added buoyant force pushes the fluid stream with higher velocity in the upward direction. This ensures a more distributed flow over the heaters, and thus, it provides more efficient heat transfer performance.

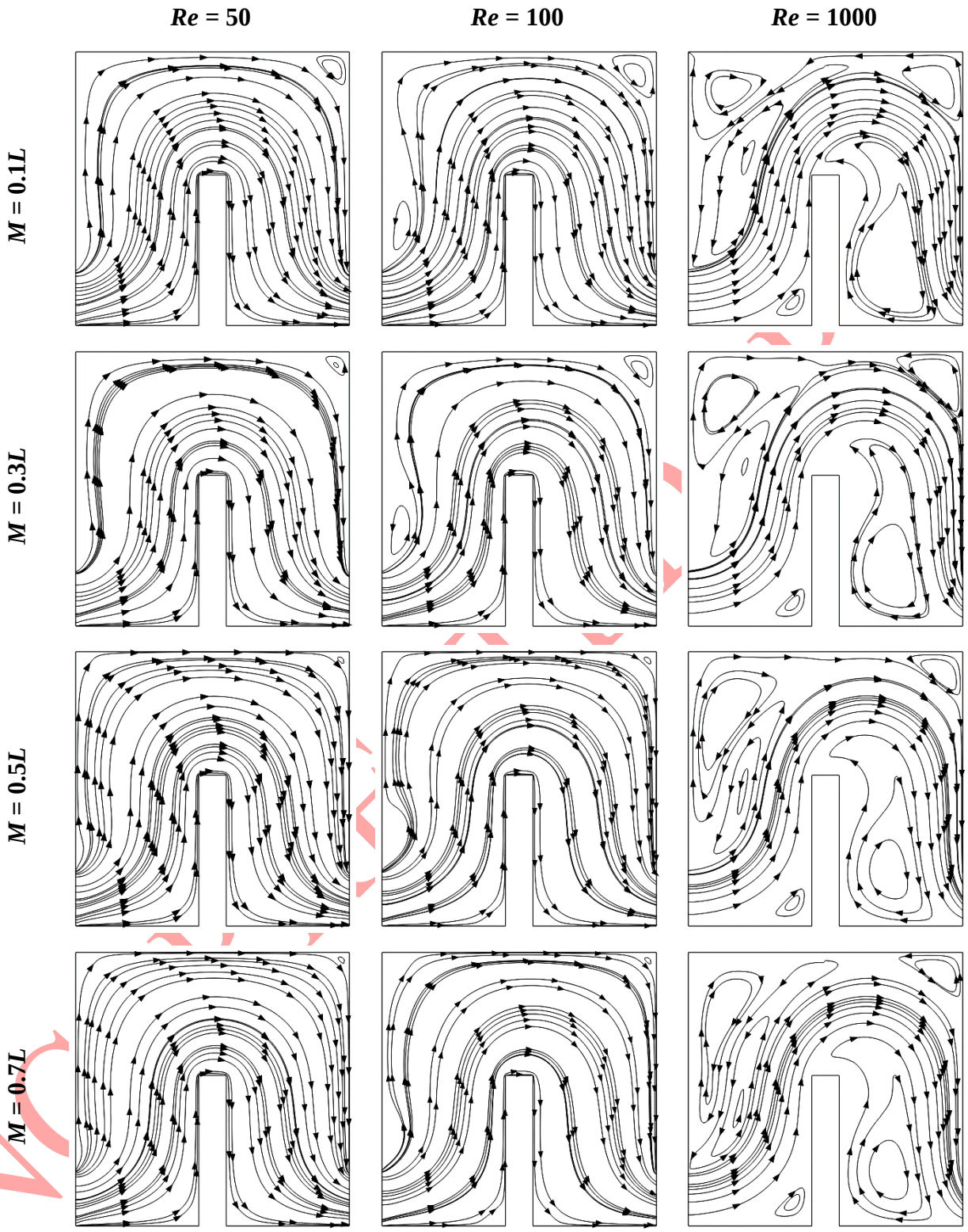

Fig. 6: Illustration of flow field for several combinations of Reynolds number and heaters location (color online).

5.2 Analysis of The Thermal Field

The isotherms are generated to visualize the temperature distribution in the flow domain, as shown in Fig. 7 and Fig. 8, for the same combinations considered in the velocity field. According to Fig. 7, as baffle height increases with a fixed heaters location (M = 0.5L), the distribution of the cold inlet fluid becomes more uniform, and thus, the heat transfer rate increases. This occurrence can be confirmed by observing the increased density of the low temperature isotherms for higher baffle height cases. Similarly, with the advantage of better distribution of the working fluid by higher baffle heights (> 0.25L), the increase in Reynolds number causes the increase in the number of low temperature isotherms due to the augmentation of flow rate. However, an interesting phenomenon is observed when Reynolds number is increased for lower baffle heights (< 0.25L). For those cases, although, the increase of Re can improve the heat transfer rate, the number of low temperature isotherms do not increase to that extent. This is due to the lack of proper distribution of the flowing fluid.

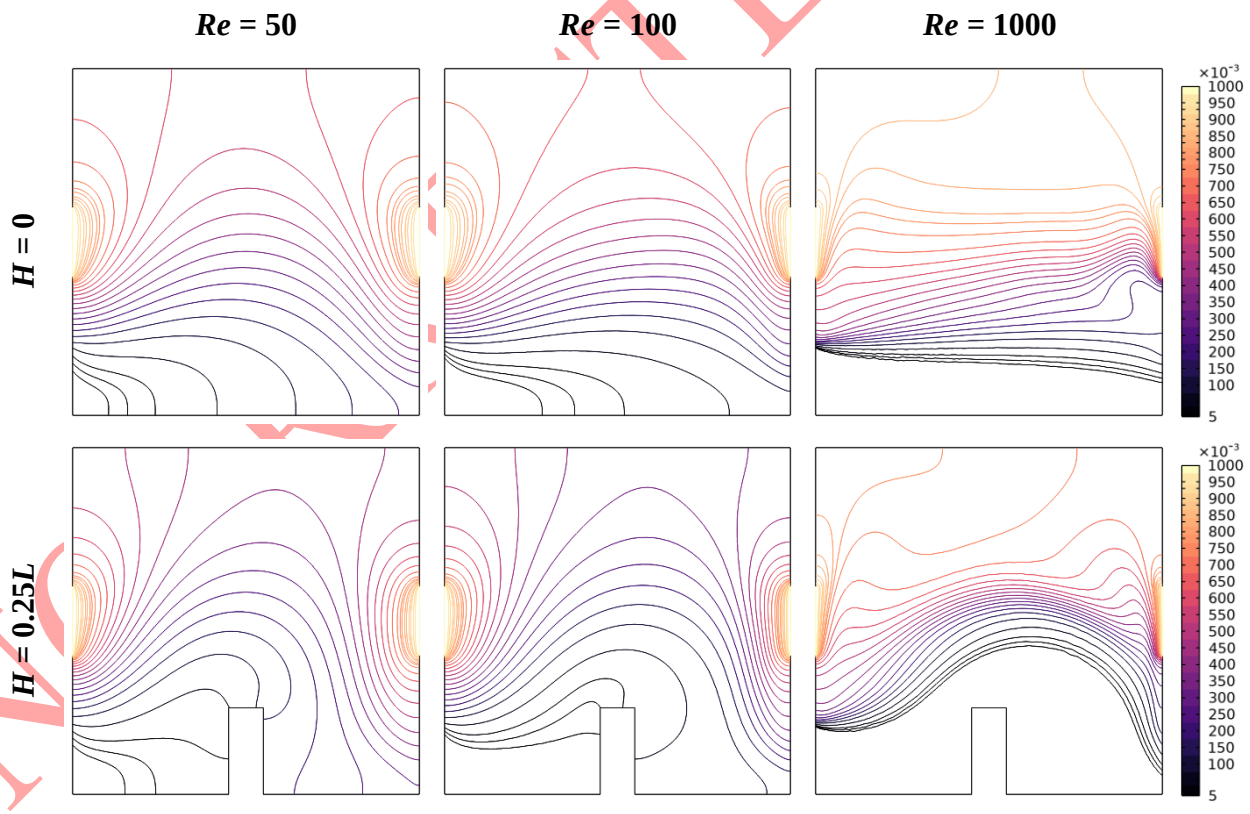

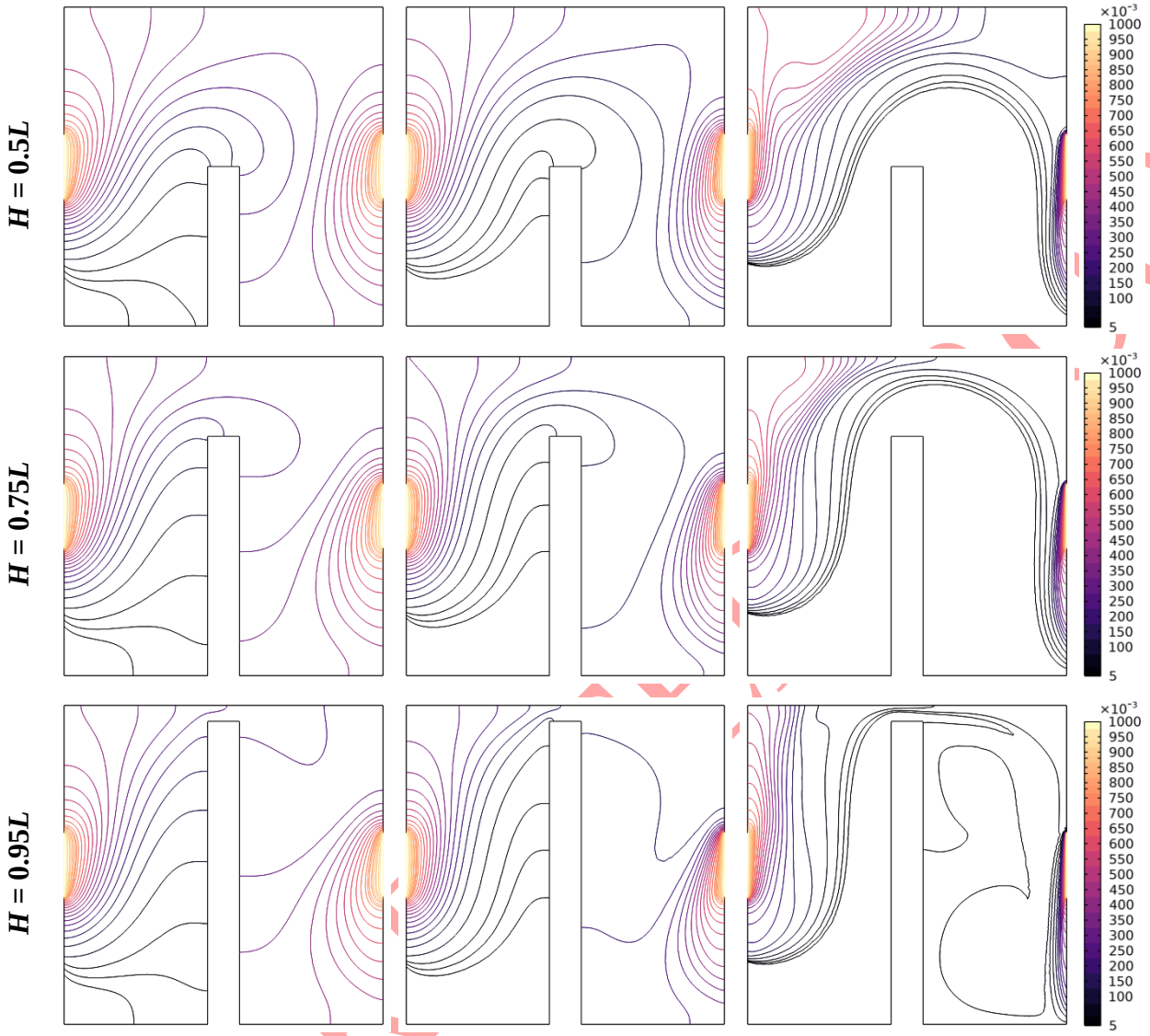

Fig. 7: Illustration of flow field for several combinations of Reynolds number and baffle height (color online).

Later, the distribution of the isotherms is presented in Fig. 8 for a constant baffle height of 0.55*L* by varying the heater's location. The placement of the heater close to the inlet allows the bulk fluid taking the heat earlier and getting enough time to distribute it as much as possible. The isotherms plot also confirms the phenomenon for the entire range of *Re*. This proper distribution of heat for $M = 0.7L$ ensures that maximum portion of the mainstream flow is participating in the heat transfer process. For the same reason, the right heating element can also encounter a greater amount of heat transfer.

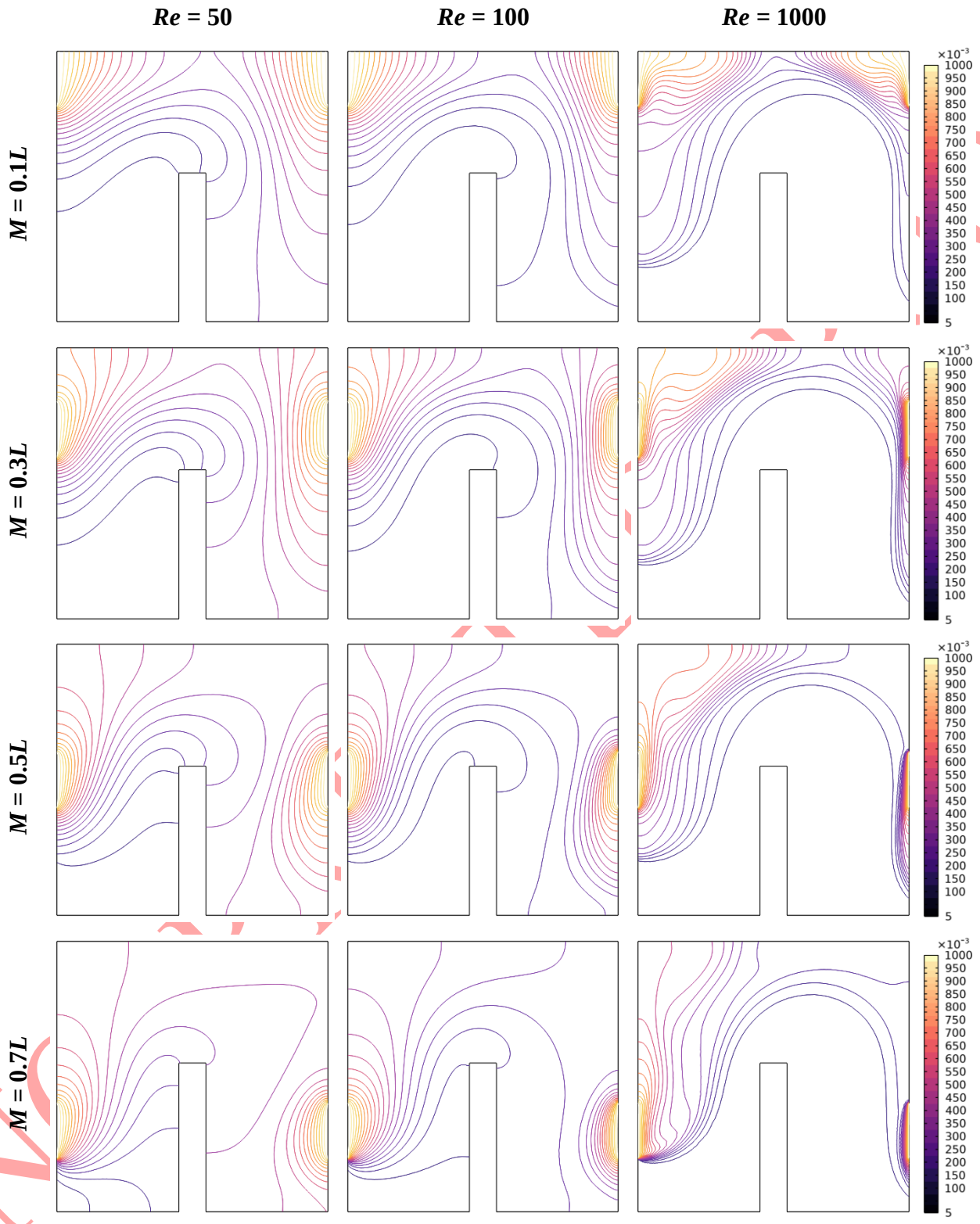

Fig. 8: Illustration of flow field for several combinations of Reynolds number and baffle height (color online).

5.3 Effect of The Variation of Baffle Height, Heater Location and Reynolds Number

Initially, to compare the heat transfer performance and overall economy, the variation of average fluid temperature, average value of Nusselt number, drop in pressure, and performance index with the rise of baffle height are plotted in Fig. 9. In these cases, heater's location remains constant at $M = 0.5L$. In Fig. 9(a), it is observed that the average temperature of the domain decreases with the increase of baffle height for the entire range of Reynolds number. Now, in comparison between different Reynolds numbers, the average temperature is found to be lesser for the lower values of *Re* mentioning that *H* is approximately lower than $0.25L$. It might seem contradictory with the low heat transfer rate by the reduced values of *Re*. However, this can be explained by observing the thermal field that the uniform distribution of the working fluid makes the average temperature a bit lower while maintaining a poorer heat transfer rate. For baffle height larger than $0.25L$, mean temperature of the cavity gets reduced in case of increasing value of Reynolds number. This effect arises from the amalgamated effect of high flow rate and guided flow. In case of heat transfer performance (Fig. 9(b)), the average value of Nusselt number monotonously increases with the increase of Reynolds number whatever the baffle height is lower or higher. When baffle height increases for a fixed Reynolds number, working fluid starts distributing along the heat-generating elements. The guidance can also be confirmed by visualizing the flow field. This guided distribution of the flow is mainly responsible for the enhancement of heat transfer performance and the average Nusselt number. On the other hand, for certain baffle height, such as $H = 0.5L$, the average Nusselt number does not exceed 20 for *Re* less than 100. However, for $Re = 1000$, it reaches up to 54 despite the fact that heaters temperature is unchanged. At higher Reynolds number, increased value of mass flow rate helps in reducing the bulk fluid temperature and increasing the temperature gradient. Since it is a direct function of temperature gradient, the average Nusselt number can reach to such higher values.

Addition of baffle causes hindrance to the flow resulting in a significant increase in pressure drop, despite its efficient removal of heat from heaters. From Fig. 9(c), it is apparent that pressure drop increases with the increment of baffle height and Reynolds number. Higher Reynolds number indicates the increase in inlet velocity which leads to the rise in velocity gradient along the walls. Since wall shear stress is directly proportional to the velocity gradient, it causes an additional pressure drop in the system. To incorporate the magnification of heat transfer and pressure drop with the rise of *H* and *Re*, it is very crucial to conduct an economic analysis to find

the most efficient geometrical and flow conditions. To do so, the performance index is evaluated for the entire range of the governing parameters and plotted in Fig. 9(d). It can be contemplated from the figure that the moderate values of H (~0.5) and Re (~100) are the most economic conditions and these can increase the overall performance by approximately 35% compared to the no baffle condition. Another important phenomenon is observed that the performance index reaches to a minimum value for $H = 0.25L$ and $Re = 1000$. At this baffle height, mainstream flow is severely interfered by the additionally formed vortices due to the adverse solid-fluid interaction. This interaction is responsible for higher pressure drop than the increase of heat transfer. Thus, the performance index becomes lower at this configuration.

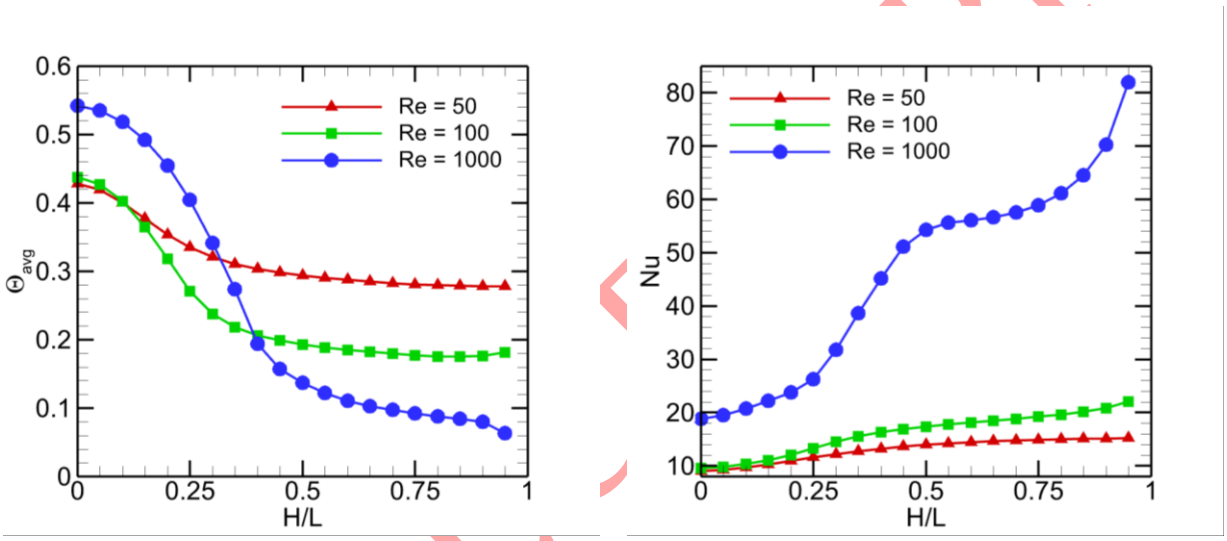

(a) (b)

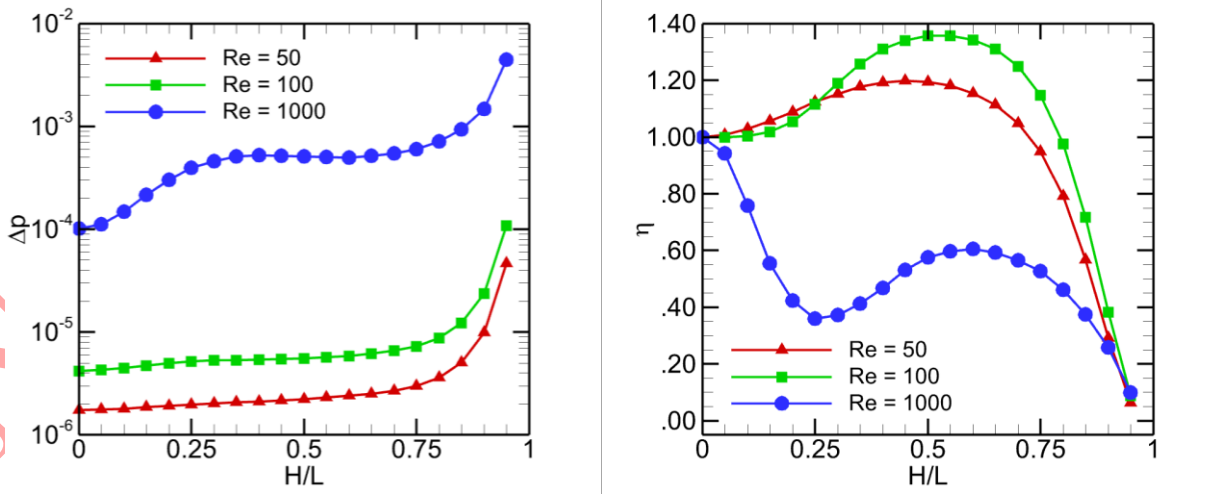

(c) (d)

Fig. 9: Effect of the variation of H/L and Re in (a) average temperature of the domain, (b) average value of Nusselt number, (c) drop in pressure, and (d) performance index (color online).

Later, the similar performance parameters are calculated by changing the location of the heaters while keeping the baffle height at $0.55L$. In Fig. 10(a), it is apparent that the average temperature gradually increases as the heaters are placed close to the inlet and outlet for the lower values of Re (50 and 100). This occurs because majority of the mainstream flow participates in heat transfer and distributes the temperature. However, for Re = 1000, this distribution effect is predominated by the high heat transfer rate with the increase amount of mass flow rate, and thus, average temperature starts decreasing for $M > 0.2$. However, the average Nusselt number increases monotonously, as shown in Fig. 10(b), since heat transfer rate increases as the heaters come closer to the inlet and outlet for the entire range of Re. On the other hand, the pressure drop seems to be the function of Re only since the obstruction causes by the baffle is not changing. The effect is demonstrated in Fig. 10(c). The combined effect of pressure head loss and heat transfer performance is shown in Figure 10(d). The figure insists that it is wise to place the heater close to the inlet and outlet ($M = 0.7L$) since it can provide 58.41% augmentation in heat transfer. Also, there is a moderate value of Re for which the system operates most economically.

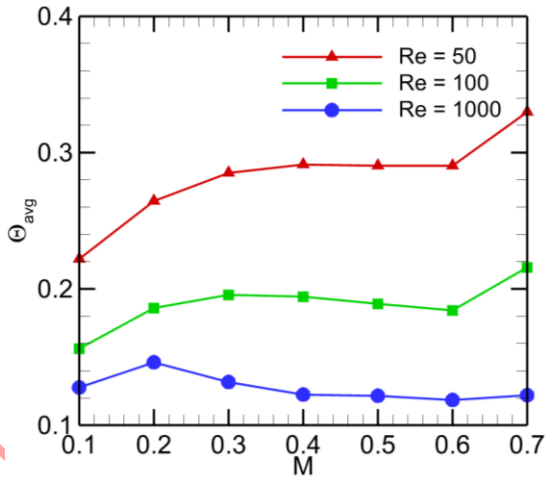

(a)

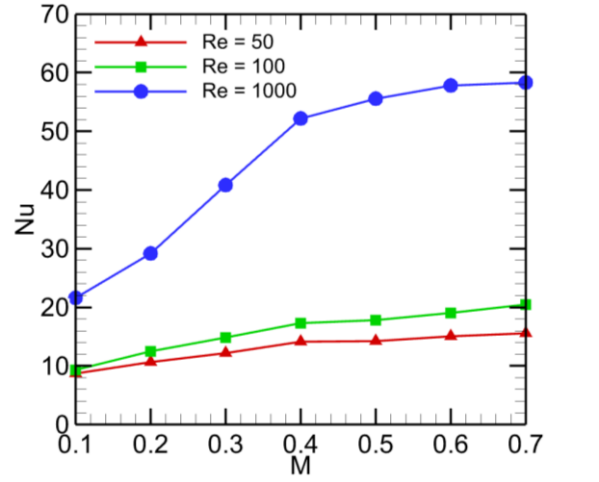

(b)

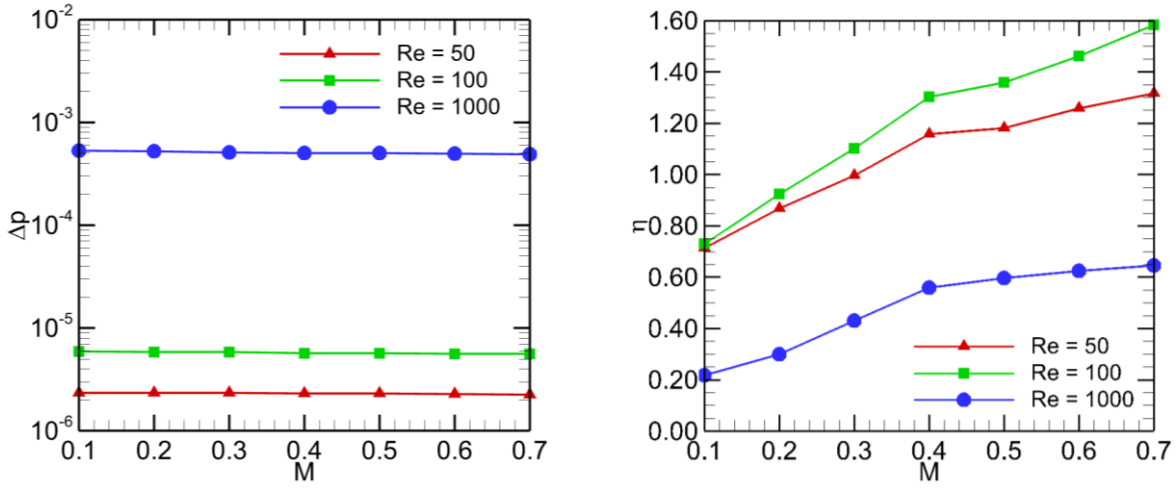

(c) (d)

Fig. 10: Effect of the variation of *M* and *Re* in (a) average temperature of the domain, (b) average value of Nusselt number, (c) drop in pressure, and (d) performance index (color online).

To evaluate the exact economic condition, a set of data is accumulated in Table 2 by taking the maximum performance index for each baffle height and its corresponding Reynolds number. It can be summarized that the optimum baffle height is 0.55*L* and the optimum Reynolds number is 100 with an increase in performance by 35.75%. Moreover, a wide range of baffle height (0.4*L* to 0.8*L*) can perform better if the Reynolds number is maintained at 100. Subsequently, for this optimum baffle height (H = 0.55*L*), another set of data is tabulated in Table 3 by changing the position of the heaters. It shows that for the same values of *Re*, a maximum amount of 58.41% enhancement of performance can be utilized if the heaters are placed next to the inlet and outlet vents.

Table 2: Values of maximum performance index (η_{max}) for each baffle height.

H/L	η_{max}	**Corresponding *Re***
0	1	-
0.05	1.008306011	50
0.1	1.028381781	50
0.15	1.058723516	60

0.2	1.097064261	70
0.25	1.1501107	70
0.3	1.20483673	80
0.35	1.261733908	90
0.4	1.309672264	100
0.45	1.340697943	100
0.5	1.356626444	100
0.55	**1.357528857**	**100**
0.6	1.342330773	100
0.65	1.310135438	100
0.7	1.248472374	100
0.75	1.146329192	100
0.8	0.975681577	100
0.85	0.722305541	200
0.9	0.409485862	200

Table 3: Values of maximum performance index (η_{max}) for different heater location at optimum baffle height.

M/L	η_{max}	**Corresponding *Re***
0.1	0.738994838	80
0.2	0.926673622	90
0.3	1.101369111	100
0.4	1.302929991	100
0.5	1.357528857	100
0.6	1.461288393	100
0.7	**1.584141035**	**100**

5.4 Performance of Optimum Baffle Height and Heaters location at Various Reynolds Number

Finally, the overall performance of the optimum geometric condition is plotted in Fig 11. It is seen in Fig. 11(a) that the average temperature of the domain exponentially decreases with the increase of *Re*. The *Nu* also increases for the entire range of *Re*, as depicted in Fig. 11(b), with a note that the performance of left wall does not increase much due to the formation of vortices and the separation of flow. However, the demonstration in Fig. 11(c) shows that the augmented pressure drop will be a limiting factor for the economic operation of the system. Lastly, the illustration of performance index in Fig. 11(d) revealed that this optimum configuration can perform better than the no baffle condition if the *Re* lies between 20 to 400.

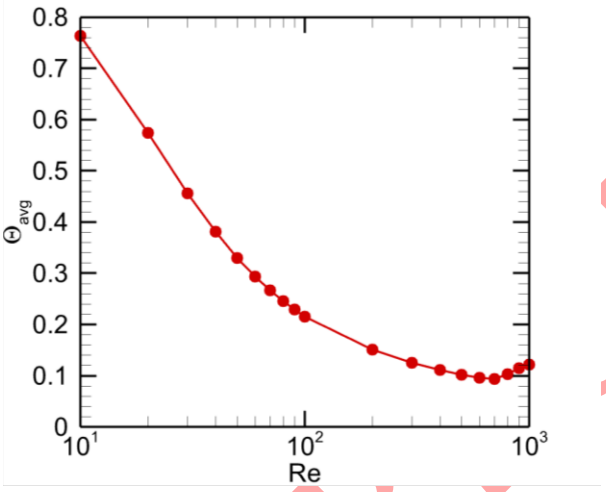

(a)

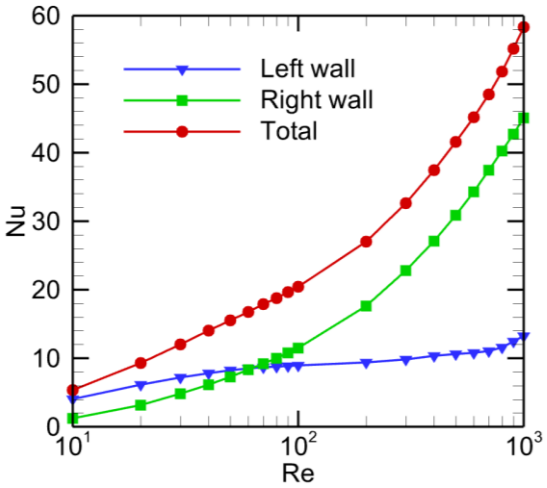

(b)

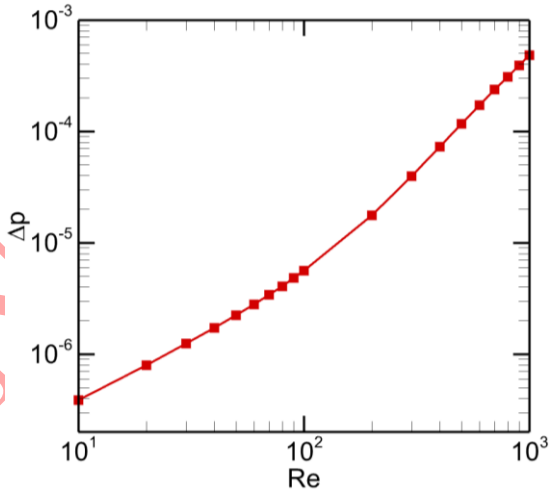

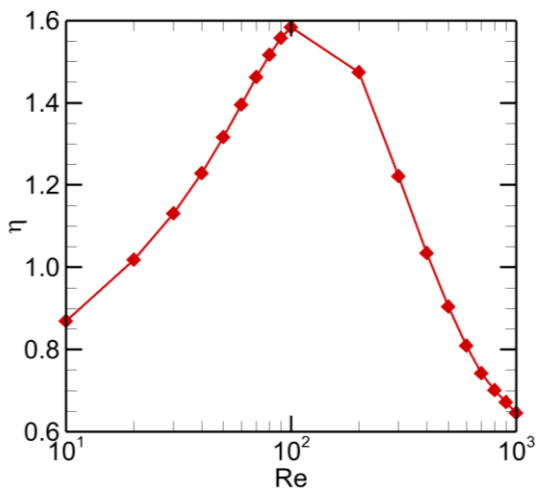

(c) (d)

Fig. 11: Effect of the variation of *Re* in (a) average temperature of the domain, (b) average value of Nusselt number, (c) drop in pressure, and (d) performance index for the optimum baffle height ($H = 0.55L$) and heaters location ($M = 0.7L$) (color online).

6. Conclusion

In this article, the most economic baffle height, heater's location and Reynolds number have been evaluated for mixed convective discrete heating elements. After a thorough qualitative inspection, the optimum conditions have been selected based on different performance parameters, such as average temperature of the domain, Nu, Δp and η. The overall output of the study can be summarized as:

- The increase of baffle height and Reynolds number causes a gradual increase in both the heat transfer performance and the pressure drop.
- Up to a critical baffle height, the average temperature of the domain increases with the rise of *Re* due to the improper distribution of the working fluid.
- Additionally, the system performs better if the heaters can be set closest to the inlet and outlet vents.
- The optimum baffle height and heater's distance from the upper wall are $0.55L$ and $0.7L$, respectively, at $Re = 100$. It provides an increase in performance by 58.41%.
- According to the performance indices, the optimum baffle height and heater's location can provide economic heat transfer performance for the range of $20 < Re < 400$.

This investigation is limited to uniform laminar flow regime only. However, the findings of this numerical analysis can work as an intuitive ground in the extension of the study by considering turbulent flow regime with different inlet profile (e.g., Poiseuille, Couette), nanofluid, iso-flux heating elements, and so on. In addition to this, phase-change material can be utilized here to take the advantage of higher latent heat in the heat transfer enhancement.

Acknowledgements

The authors would like to show their profound gratitude to Dr. Sumon Saha, Professor, Department of Mechanical Engineering, BUET and CFDHT Research Group.

Nomenclature

Roman Symbols	Greek Symbols
A: Area	α: Thermal diffusivity (m^2/s)
g: Gravitational acceleration (m/s^2)	β: Coefficient of volume expansion (1/K)
H: Non - dimensional height	η: Performance index
L: Non - dimensional length	Θ: Non – dimensional temperature
M: Distance of the heater from top end	υ: Kinematic viscosity
N: Normal to the surface	
Nu: Nusselt number	Subscripts
p: Pressure (Pa)	avg: Average
P: Non - dimensional pressure	c: cold
Pr: Prandtl number	h: hot
Re: Reynolds number	in: Inlet
Ri: Richardson number	Subscripts
T: Temperature (K)	
u, v: Velocity components (m/s)	
U, V: Non – dimensional velocity components	
X, Y: Non – dimensional cartesian coordinates	

References

[1] Y.A. Cengel, A.J. Ghajar, Heat and Mass Transfer, 5th ed., McGraw-Hill Education, New York, 2015.

[2] G. de Vahl Davis, Natural convection of air in a square cavity: a bench mark numerical solution., Int. J. Numer. Methods Fluids. 3 (1982) 249–264. https://doi.org/https://doi.org/10.1002/fld.1650030305.

[3] B. Gebhart, T. Freeman, S. Lecture, Buoyancy Inlucel Fluid Motions Characteristic of Applications in Technology, Trans. ASME. 101 (1979) 5–28.

[4] L. Iyican, L.C. Witte, Y. Bayazitoğlu, An experimental study of natural confection in trapezoidal enclosures, J. Heat Transfer. 102 (1980) 648–653. https://doi.org/10.1115/1.3244366.

[5] Y.E. Karyakin, Y.A. Sokovishin, O.G. Martynenko, Transient natural convection in triangular enclosures, Int. J. Heat Mass Transf. 31 (1988) 1759–1766. https://doi.org/10.1016/0017-9310(88)90190-1.

[6] S. Ostrach, Natural Convection in Enclosures, J. Heat Transfer. 110 (1988) 1175–1190.

https://doi.org/https://doi.org/10.1115/1.3250619.

[7] R.A. Kuyper, T.H. Van Der Meer, C.J. Hoogendoorn, R.A.W.M. Henkes, Numerical study of laminar and turbulent natural convection in an inclined square cavity, Int. J. Heat Mass Transf. 36 (1993) 2899–2911. https://doi.org/10.1016/0017-9310(93)90109-J.

[8] W.H. Leong, K.G.T. Hollands, A.P. Brunger, Experimental Nusselt numbers for a cubical-cavity benchmark problem in natural convection, Int. J. Heat Mass Transf. 42 (1998) 1979–1989. https://doi.org/10.1016/S0017-9310(98)00299-3.

[9] S. Singh, M.A.R. Sharif, Mixed convective cooling of a rectangular cavity with inlet and exit openings on differentially heated side walls, Numer. Heat Transf. , Part A Appl. An Int. J. Comput. Methodol. 44 (2003) 233–253. https://doi.org/http://dx.doi.org/10.1080/716100509.

[10] B. Calcagni, F. Marsili, M. Paroncini, Natural convective heat transfer in square enclosures heated from below, Appl. Therm. Eng. 25 (2005) 2522–2531. https://doi.org/10.1016/j.applthermaleng.2004.11.032.

[11] A. Raji, M. Hasnaoui, Mixed convection heat transfer in a rectangular cavity ventilated and heated from the side, Numer. Heat Transf. , Part A Appl. An Int. J. Comput. Methodol. 33 (1998) 533–548. https://doi.org/http://dx.doi.org/10.1080/10407789808913953 PLEASE.

[12] D. Angirasa, Mixed convection in a vented enclosure with an isothermal vertical surface, Fluid Dyn. Res. 26 (2000) 219–233. https://doi.org/10.1016/S0169-5983(99)00024-6.

[13] C.L. Chen, C.H. Cheng, Experimental and numerical study of mixed convection and flow pattern in a lid-driven arc-shape cavity, Heat Mass Transf. Und Stoffuebertragung. 41 (2004) 58–66. https://doi.org/10.1007/s00231-004-0541-5.

[14] S. Saha, A.H. Mamun, M.Z. Hossain, A.K.M.S. Islam, Mixed Convection in an Enclosure with Different Inlet and Exit Configurations, J. Appl. Fluid Mech. 1 (2008) 78–93. https://doi.org/10.36884/jafm.1.01.11840.

[15] A.J. Chamkha, S.H. Hussain, Q.R. Abd-Amer, Mixed convection heat transfer of air inside a square vented cavity with a heated horizontal square cylinder, Numer. Heat Transf. Part A Appl. 59 (2011) 58–79. https://doi.org/10.1080/10407782.2011.541216.

[16] M.M. Rahman, S. Parvin, R. Saidur, N.A. Rahim, Magnetohydrodynamic mixed convection in a horizontal channel with an open cavity, Int. Commun. Heat Mass Transf. 38 (2011) 184–193. https://doi.org/10.1016/j.icheatmasstransfer.2010.12.005.

[17] S.K. Ajmera, A.N. Mathur, Experimental investigation of mixed convection in multiple ventilated enclosure with discrete heat sources, Exp. Therm. Fluid Sci. 68 (2015) 402–411. https://doi.org/10.1016/j.expthermflusci.2015.05.012.

[18] F. Garoosi, G. Bagheri, M.M. Rashidi, Two phase simulation of natural convection and mixed convection of the nanofluid in a square cavity, Powder Technol. 275 (2015) 239–256. https://doi.org/10.1016/j.powtec.2015.02.013.

[19] J. Burgos, I. Cuesta, C. Salueña, Numerical study of laminar mixed convection in a square open cavity, Int. J. Heat Mass Transf. 99 (2016) 599–612. https://doi.org/10.1016/j.ijheatmasstransfer.2016.04.010.

[20] S.A.M. Mehryan, E. Izadpanahi, M. Ghalambaz, A.J. Chamkha, Mixed convection flow caused by an oscillating cylinder in a square cavity filled with Cu–Al2O3/water hybrid nanofluid, J. Therm. Anal. Calorim. 137 (2019) 965–982. https://doi.org/10.1007/s10973-019-08012-2.

[21] E. Çolak, Ö. Ekici, H.F. Öztop, Mixed convection in a lid-driven cavity with partially heated porous block, Int. Commun. Heat Mass Transf. 126 (2021). https://doi.org/10.1016/j.icheatmasstransfer.2021.105450.

[22] T.H. Ruvo, S. Saha, S. Mojumder, S. Saha, Mixed convection in an open T-shaped cavity utilizing the effect of different inflow conditions with Al2O3-water nanofluid flow, Results Eng. 17 (2023) 100862.

[23] I. Kotcioğlu, T. Ayhan, H. Olgun, B. Ayhan, Heat transfer and flow structure in a rectangular channel with wing-type vortex generator, Turkish J. Eng. Environ. Sci. 22 (1998) 185–195.

[24] A. Valencia, M. Sen, Unsteady flow and heat transfer in plane channels with spatially periodic vortex generators, Int. J. Heat Mass Transf. 46 (2003) 3189–3199. https://doi.org/10.1016/S0017-9310(03)00099-1.

[25] R. Karwa, B.K. Maheshwari, N. Karwa, Experimental study of heat transfer enhancement in an asymmetrically heated rectangular duct with perforated baffles, Int. Commun. Heat Mass Transf. 32 (2005) 275–284. https://doi.org/10.1016/j.icheatmasstransfer.2004.10.002.

[26] T. V. Radhakrishnan, G. Joseph, C. Balaji, S.P. Venkateshan, Effect of baffle on convective heat transfer from a heat generating element in a ventilated cavity, Heat Mass Transf. Und Stoffuebertragung. 45 (2009) 1069–1082. https://doi.org/10.1007/s00231-008-0474-5.

[27] M.A. Belmiloud, N. eddine S. chemloul, Effect of baffle number on mixed convection within a ventilated cavity, J. Mech. Sci. Technol. 29 (2015) 4719–4727. https://doi.org/10.1007/s12206-015-1019-8.

[28] A.K. Sharma, P.S. Mahapatra, N.K. Manna, K. Ghosh, Mixed Convection Heat Transfer in a Grooved Channel in the Presence of a Baffle, Numer. Heat Transf. Part A Appl. 67 (2015) 1097–1118. https://doi.org/10.1080/10407782.2014.955359.

[29] D. Sahel, H. Ameur, R. Benzeguir, Y. Kamla, Enhancement of heat transfer in a rectangular channel with perforated baffles, Appl. Therm. Eng. 101 (2016) 156–164. https://doi.org/10.1016/j.applthermaleng.2016.02.136.

[30] M.A. Belmiloud, N. Sad_Chemloul, M. Guemmour, Effect of baffle length on mixed convection coupled to surface radiation in a rectangle cavity, J. Renew. Energies. 20 (2017) 81–89. https://doi.org/10.54966/jreen.v20i1.611.

[31] P. Gokulavani, M. Muthtamilselvan, Q.M. Al-Mdallal, D.H. Doh, Effects of orientation of the centrally placed heated baffle in an alternative configured ventilation cavity, Eur. Phys. J. Plus. 135 (2020) 1–16. https://doi.org/10.1140/epjp/s13360-019-00070-7.

[32] Z.A. Alhussain, Mixed convective flow in a multiple port ventilation square cavity with insulated baffle, Case Stud. Therm. Eng. 30 (2022) 101785. https://doi.org/10.1016/j.csite.2022.101785.

[33] N. Rehman, R. Mahmood, A. Hussain, M.R. Ali, A.S. Hendy, Case Studies in Thermal Engineering Enhanced heat transfer in vented square enclosures with block structures : Exploring iso-perimetric shapes and multigrid approach for mixed convection of nano-fluids, Case Stud. Therm. Eng. 58 (2024) 104391. https://doi.org/10.1016/j.csite.2024.104391.

[34] F.T. Mahmood, T.S. Chowdhury, M.N. Hasan, Fluid-structure interaction induced mixed convection characteristics in a lid-driven square cavity with non-Newtonian power law fluids, Int. J. Thermofluids. 22 (2024) 100687. https://doi.org/10.1016/j.ijft.2024.100687.

[35] M.N. Hasan, S. Saha, M.N. Hasan, S. Barua, Influence of active flow modulation on conjugate mixed convection inside a vented cavity, Proc. Inst. Mech. Eng. Part C J. Mech. Eng. Sci. 236 (2022) 6923–6938. https://doi.org/10.1177/09544062211068731.

[36] M.M. Derakhshan, M.A. Akhavan-Behabadi, S.G. Mohseni, Experiments on mixed convection heat transfer and performance evaluation of MWCNT-Oil nanofluid flow in horizontal and vertical microfin tubes, Exp. Therm. Fluid Sci. 61 (2015) 241–248. https://doi.org/10.1016/j.expthermflusci.2014.11.005.